

Interaction between hydrophobic surfaces with metastable intervening liquid

D. Bratko,^{a)} R. A. Curtis, H. W. Blanch, and J. M. Prausnitz

Department of Chemical Engineering, College of Chemistry, University of California, Berkeley, California 94720 and Chemical Sciences Division, Lawrence Berkeley National Laboratory, Berkeley, California 94720

(Received 26 April 2001; accepted 31 May 2001)

Molecular simulation is used to elucidate hydrophobic interaction at atmospheric pressure where liquid water between apolar walls is *metastable* with respect to capillary evaporation. The steep increase of the estimated activation barrier of evaporation with surface–surface separation explains the apparent stability of the liquid at distances more than an order of magnitude below the thermodynamic threshold of evaporation. Solvation by metastable liquid results in a short-ranged oscillatory repulsion which gives rise to an irreversible potential barrier between approaching walls. The barrier increases with external pressure in accord with measured pressure-induced slowing of conformational transitions of biopolymers with strong hydrophobic interactions. At a sufficiently small separation, the force abruptly turns attractive signaling nucleation of the vapor phase. This behavior is consistent with the cavitation-induced hysteresis observed in a number of surface–force measurements for strongly hydrophobic surfaces at ambient conditions. © 2001 American Institute of Physics. [DOI: 10.1063/1.1386926]

I. INTRODUCTION

Hydrophobic effects influence a wide range of molecular phenomena in aqueous solutions, from gas solubility to detergency, formation of membranes, and protein folding.¹ Attractive interaction between extended hydrophobic solutes is associated with surface dewetting which occurs below a critical interparticle separation, d_c . Within a coarse-grained description and for planar geometry, d_c is approximately given by the Kelvin equation $d_c \sim 2(\gamma_{wl} - \gamma_{wv})/\rho\Delta\mu$, where ρ is the liquid number density, $\Delta\mu$ is the difference of the chemical potential of the liquid from liquid/gas coexistence value, γ is the interfacial free energy, and subscripts w , l , and v denote the walls and the intervening liquid or vapor phase, respectively. For strongly hydrophobic solutes and ambient conditions, with the bulk pressure $P_b = 1$ atm, and $\rho\Delta\mu \sim P_b$, the distance d_c below which the vapor phase is favored is of the order of 10^3 Å.^{2–6}

Spontaneous cavitation of water between hydrophobic surfaces has long been discussed in the context of measurable surface forces.^{7–9} While a number of surface-force apparatus measurements reveal capillary evaporation between apolar surfaces, others point to the presence of liquid water at separations much smaller than allowed by the Kelvin equation.^{10–13} The presence of liquid water in narrow apolar confinement is rationalized by kinetic arguments,^{4,8,14–17} in addition to liquid-stabilizing effects of finite lateral size⁴ and partial hydrophilicity¹⁶ of the surfaces. In theoretic analyses, similar metastabilities have been considered in contexts of simple fluids,^{18–21} and also water in a wetting confinement,²² but not for the drying scenario of our present interest. Continuum-analytic calculations^{8,14,15} and simulations for

coarse-grained^{4,17} waterlike models predicted the existence of an activation barrier separating the vapor and liquid phases. The barrier can be sufficiently high to lead to the metastability of the liquid phase over experimentally relevant times^{10–13} unless the wall–wall separation is reduced to a few [O(10)] molecular layers.¹⁷ Interpretations of kinetic aspects of hydrophobicity, including the well known hysteresis in surface-force-apparatus measurements,^{10–12} thus warrant a molecular-level description which has so far not been provided.

Molecular simulation studies have elucidated several features of confined water.^{13,23–39} However, many of these studies were concerned with hydrophilic confinements, and only a few were performed using open (constant pressure or chemical potential) ensemble suitable to consider capillary evaporation or equilibrium with bulk liquid. The first simulation study of confined water performed in the *open* ensemble (GCMC), used³⁶ the BBL model of water⁴⁰ (surface tension, γ_{lv} , close to 50 mJ/m²) between parallel hard walls at bulk pressure $P_b \sim 2 \times 10^3$ atm. Evaporation was observed at wall–wall distances d below about 5 Å, a value close to the estimate from the Kelvin equation (approximately valid²¹ at given d). Similarly, the isotonic ensemble simulations for SPC model of water, also between hard walls and at $P_b \sim 1.5 \times 10^3$ atm, have shown evaporation below $d \sim 10$ Å.¹³ Due to the small value of d_c at high external pressure (large $\Delta\mu$) considered in these two studies, the observed liquid phase in contact with hard walls was thermodynamically stable. At low pressure, $P_b < 10$ atm, on the other hand, the simulations of SPC and SPC/E water between hard walls that we performed at the preliminary stage of this work, resulted in evaporation at all trial separations, d . Molecular dynamics simulation of water between hard ellipsoids of lateral size of about 18 Å at ambient pressure showed evaporation at the

^{a)}Electronic mail: db@lolita.cchem.berkeley.edu

wall–wall distance of ~ 1 – 2 molecular layers.³⁷ This result, again, is close to the estimate from the Kelvin equation when used in its generalized form⁴ that accounts for the reduction of d_c due to finite lateral size of the confinement.

In the present article, we report the first *ambient pressure* results obtained in systematic open (Grand Canonical) ensemble simulations for the structure and for the solvation force between apolar plates with weak wall/water attraction that mimics hydrocarbon surfaces.³⁵ We consider separations from contact to 60 \AA . For bulk pressure $P_b = 0 \pm 10 \text{ atm}$ we identify slit widths where liquid water persists in an initially filled pore in a metastable state. Molecular simulation is used to estimate the free energy barrier (for a set of distances) that prevents or slows capillary evaporation. We also consider situations when the liquid phase is stabilized by elevated pressure $P_b \sim 10^3 \text{ atm}$. We show that the potential between approaching hydrophobic domains separated by *metastable* liquid features a maximum which has to be crossed before the surfaces are attracted to contact. The peak increases with external pressure in a similar way as the drying barrier for the *reversible* interaction of apolar solutes or residues of smaller size.^{41,42}

II. MODEL AND METHOD

We study the behavior of three-point, SPC model of water⁴³ confined between smooth parallel walls. In the absence of the confinement and at ambient temperature and pressure, SPC water whose critical temperature is $\sim 589 \text{ K}$, is known to exist in a stable liquid state.⁴⁴ The walls of the confinement mimic a hydrophobic material with integrated Lennard-Jones (9-3) interaction between a wall and the oxygen atom of water located at distance z_{iw} from the surface,

$$u_{iw}(z_{iw}) = a/z_{iw}^9 - c/z_{iw}^3, \quad (1)$$

where $a = 4\pi\rho\epsilon\sigma^{12}/45 = 2.7 \times 10^{-17} \text{ J \AA}^9$, $c = 15a/2\sigma^6 = 1.265 \times 10^{-19} \text{ J \AA}^3$, ρ is the number density of C atoms of the hydrocarbon, and ϵ and σ are the Lennard-Jones parameters describing the average interaction between hydrocarbon CH_n groups and the oxygen atom of water.^{35,38} The solvation pressure, $P_s(d)$, acting on either wall at slit width d is determined as the difference between the average force per unit area exerted on the wall by all water molecules *in* the slit, $P(d)$, and bulk pressure $P_b \equiv P(\infty)$. Direct Lennard-Jones forces between opposite walls⁴⁵ add the term, $P_h \sim a' d^{-9} - c' d^{-3}$, where $a' \sim 1.04 \times 10^7 \text{ \AA}^9 \text{ atm}$, and $c' \sim 2.8 \times 10^4 \text{ \AA}^3 \text{ atm}$ corresponding to the Hamaker constant $A \equiv 6\pi c' \sim 5.3 \times 10^{-20} \text{ J}$. The sum $P_s + P_h \equiv P_t$ represents the total pressure on either wall related to measured surface forces through Derjaguin approximation.⁴⁶

Using Grand Canonical Ensemble Monte Carlo simulations,^{47,48} the confined liquid is held in an apparent equilibrium with bulk reservoir characterized by a chemical potential, μ . Two states of bulk water that we considered correspond to bulk pressures $P_b = 0 \pm 10 \text{ atm}$ or $1000 \pm 10 \text{ atm}$, densities $0.993 \pm 0.01 \text{ g cm}^{-3}$ and $1.03 \pm 0.01 \text{ g cm}^{-3}$, and reduced isothermal compressibilities, $\rho k_B T \kappa = 0.063$ (experimental value is 0.062) and 0.058, respectively. P_b corresponds to the large distance limit of the pressure acting on the inner surfaces of the walls. For SPC water

at cubic box size $L = 18 \text{ \AA}$, and for the spherical cutoff given by Eq. (2) of Ref. 38, the above two states are characterized by excess chemical potentials $\mu_{\text{ex}}/k_B T = -10.596$ at the lower, and -9.87 at the higher P_b . Clearly, the appropriate values of chemical potential depend slightly on the cutoff of the intermolecular potential, the system size, and the boundary conditions. While our code includes a two-dimensional Ewald-sum routine⁴⁹ from previous studies,⁵⁰ computer time restrictions due to slow convergence of density and pressure precluded the application of this computation intensive technique in systematic calculations. As the optimal practical alternative, we use periodic conditions in lateral directions, combined with spherical cutoff for water–water interactions described by Eq. (2) of Ref. 38. The lateral size of the simulation box, L_{xy} at small and moderate wall–wall separations, d , was held at 18 \AA . For higher d , L_{xy} was gradually increased to retain an approximately cubic shape of the water slab, reaching 36 \AA at $d = 50 \text{ \AA}$. This size of the box corresponds to $\sim 2 \times 10^3$ molecules, the most allowed by our computational resources. While not as accurate as Ewald summation,^{49,50} the above description has been shown³⁸ to be more reliable than the Minimum Image and Cylindrical-Cutoff alternatives although the truncation of the long-ranged tail in water–water potentials might slightly affect the calculated interplate force. The low pressure value of excess chemical potential we use is in reasonable agreement with the reported result, $\mu_{\text{ex}}/k_B T = -10.05 \pm 0.1$, obtained^{38,51} at almost identical conditions for bulk TIP4P model of water.⁵²

A serious difficulty in simulations of confined water is a very slow relaxation of fluctuations in liquid density profiles.^{38,53} The long-lived asymmetry in density profiles³⁸ leads to considerable differences in pressures exerted on the two walls as purely diffusive molecular motion proves insufficient for rapid equilibration. This difficulty was overcome by implementing collective moves of water molecules corresponding to simultaneous translation of all particles along the direction perpendicular to the walls. Acceptance of these moves was controlled by the usual Metropolis criterion. Including a small fraction ($\sim 1\%$) of the above collective moves resulted in rapid equilibration of density profiles and secured the symmetry of mean pressures on the two walls. While reliable calculations could not have been completed without the above modification, long runs were still necessary to obtain accurate pressure averages over the fluctuating number of molecules in the system. With straightforward GCMC acceptance of particle exchange typically around 0.015% (up to four times higher in very narrow liquid film), the time required to reduce the statistical error in solvation pressure to about 10 atm is $\sim 5.10^6$ attempted moves *per particle* or close to 10^9 attempted moves for a typical run. Using a configuration-bias technique for particle exchange⁴⁸ with only three trial orientations, the acceptance is increased by about a factor of 2.

III. RESULTS AND DISCUSSION

In Fig. 1(a) we present density profiles in confined liquid films for a wide range of slit widths at fixed chemical potential corresponding to the ambient pressure, $P_b = 0 \pm 10 \text{ atm}$. For wall–wall separations $d > 13.5 \text{ \AA}$, we find the metastable

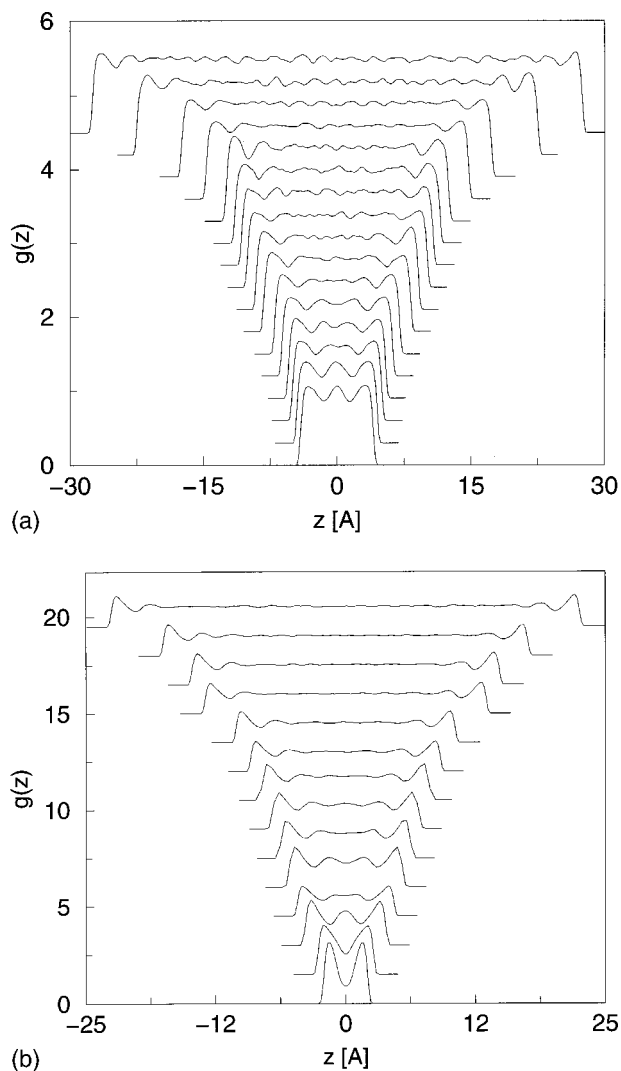


FIG. 1. Density profiles (distribution functions), $g(z)$, of oxygen atoms of water molecules in a film of metastable liquid confined between parallel hydrocarbon walls at ambient conditions (a), or at the elevated pressure $P_b \sim 10^3$ atm (b). z is the coordinate perpendicular to the walls.

liquid to persist over all practical simulation times when the initial GCMC state is a pre-equilibrated water-filled pore. Below $d \sim 12.7$ Å (about 7.9 Å accessible to centers of water molecules), we consistently observe capillary evaporation. The threshold width accommodates about three molecular layers of water. Figure 1(b) shows results from similar calculations for the high pressure, $P_b \sim 10^3$ atm. Here the liquid regularly evaporated at the threshold distance $d \sim 9$ Å (two molecular layers) which is roughly consistent with the prediction of the (equilibrium) Kelvin equation for given P_b . As d_c scales approximately as P_b^{-1} , and the accuracy of the Kelvin equation only improves with increasing d_c ,²¹ it is clear that vapor represents the thermodynamically stable state of water at the lower pressure, $P_b = 0 \pm 10$ atm, for all confinement widths d considered in our simulation.

Experimental evidence suggests the metastable liquid state is often present in realistic situations and is likely to determine the force profiles between strongly hydrophobic particles in surface-force-apparatus measurements.^{11–13} Our results pertain to this scenario and also approximately de-

scribe equilibrium situations where the liquid is stabilized^{12,4} due to finite lateral size of apolar particles.

The layering of confined liquid is most pronounced at small wall–wall distances, d , decaying with d in a weakly oscillatory manner because the density amplitudes peak at slit widths corresponding to integer multiples of molecular layers. This behavior affects the distance dependence of the solvation pressure, P_s , which varies roughly in parallel with the height of the liquid density peaks next to the walls. Beyond the separations of about six to seven molecular layers, the interfacial density profiles attain an asymptotic (single wall) form that does not change upon further increase in the wall–wall separation. This behavior differs from the recent finding of Sakurai *et al.*, where a flattening of density peaks at increased separations above $d \sim 50$ Å was observed.³⁹ The difference is, most likely, due to the use in Ref. 39 of closed (NVT) ensemble that does not provide a reliable determination of the number of water molecules as a function of the width of the slit. The present results cannot test recent theoretic predictions⁵ based on different (purely repulsive) wall/water interaction.

Figures 2(a) and 2(b) show the dependence of calculated pressure $P(d)$ on either surface as a function of the wall–wall separation, d . Despite the unavoidable statistical noise, the present results show pressure oscillations with the number of peaks roughly consistent with molecular layering of water next to the walls. Statistical errors are likely responsible for observed fluctuations in period lengths of pressure profiles. For our simulated system, the solvation pressure, $P_s = P(d) - P(\infty)$, between walls wetted by metastable intervening liquid is mostly repulsive. It gives rise to a low free energy barrier to be crossed before the liquid phase is replaced by vapor at small d . The occurrence of a qualitatively similar barrier has been occasionally indicated in measurements of surface forces between strongly hydrophobic surfaces, e.g., in Fig. 4 of Ref. 54, and in the inset of Fig. 9(b) of Ref. 55 but the origin of the effect has so far not been unambiguously identified. Apart from the differences between the experimental and model systems, direct comparisons are difficult for two reasons. On the experimental side, the presence of impurities such as dissolved gases can enable cavitation at increased interplate separations. In simulations, on the other hand, the use of a finite lateral size of the sample combined with periodic boundary conditions has been argued to produce an opposite effect.¹⁷ Computationally feasible increase of the simulation box is not sufficient to rule out eventual size effects expected only upon a major increase¹⁷ in the lateral area of the system. Integration of solvation pressure profiles shown in Fig. 2 with respect to d indicates barrier heights of ~ 5.8 and ~ 11 mJ/m² for bulk pressures of ~ 0 , and $\sim 10^3$ atm, respectively. These values are an order of magnitude smaller than the reduction in the surface free energy upon bringing the two apolar surfaces in contact.^{2,3,36,45} The pressure-induced increase in the free-energy barrier between extended apolar domains is reminiscent of the pressure effect on the potential of mean force between spherical apolar solutes considered in the framework of information theory.⁴² The theory relates the observed⁴¹ slowdown of protein conformational dynamics to

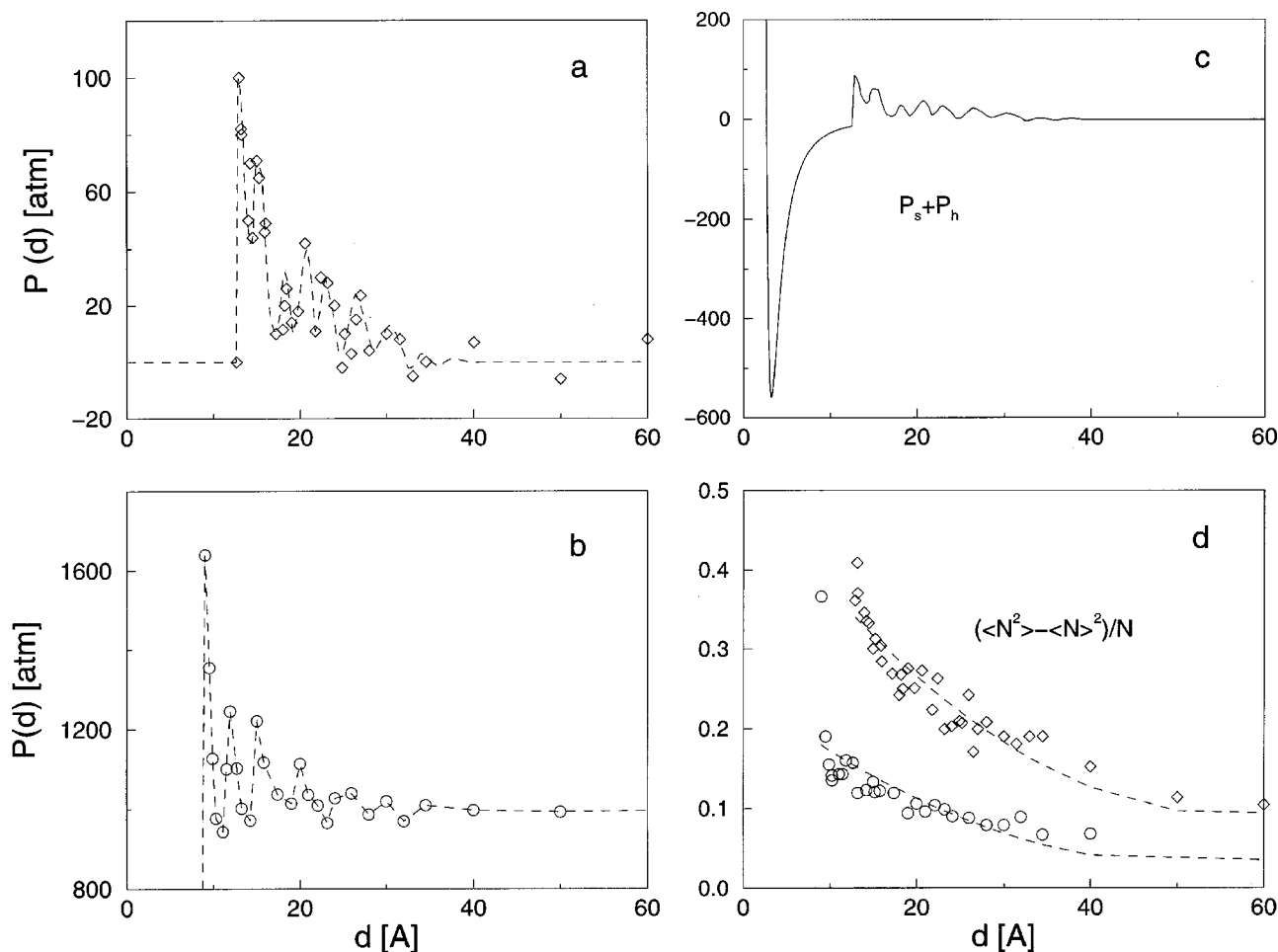


FIG. 2. Distance dependence of the pressure the confined liquid exerts on hydrocarbon walls at bulk pressure $P_b \sim 0$, or 10^3 atm (b). Statistical uncertainty for calculated pressure is about 10 atm. (c) displays the net pressure comprised of the solvation term and direct wall–wall interaction at ambient conditions. (d) shows calculated fluctuations in the number of molecules $[(N^2) - \langle N \rangle^2]/N$ as a function of the width separating the walls for $P_b \sim 0$ (diamonds) or $\sim 10^3$ atm (circles). In (a), (b), and (d), symbols denote GCMC simulation results, and dashed curves are a guide to the eye.

pressure-induced increase in the free energy barrier associated with a reversible removal (or restoring) of the aqueous film between hydrophobic residues. Despite a different mechanism, our results suggest a similar pressure dependence for the kinetics of association of exposed hydrophobic domains of partly folded protein molecules.

Figure 2(c) illustrates the distance dependence of the net pressure on the walls determined as the sum of the solvation pressure at $P_b \sim 0 \pm 10$ atm, Fig. 2(a), and the direct Lennard-Jones interaction between adjacent plates, $P_t = P_s + P_h$. Integration of the pressure curve in Fig. 2(c), however, cannot be used to estimate the wall/liquid interfacial tension as it corresponds to an irreversible process of varying the wall–wall distance; it lacks information about the free-energy drop upon the liquid–vapor transition. At elevated pressure, $P_b \sim 10^3$ atm, on the other hand, the calculated solvation pressure shown in Fig. 2(b) corresponds to a reversible or nearly reversible path. Here, integration of P_t gives the free energy change of ~ 80 mJ/m² and hence the apparent hydrocarbon/water surface tension of 40 mJ/m², a value close to experimental determinations.^{2,3}

In Fig. 2(d) we present the fluctuations in the number of molecules, $[(N^2) - \langle N \rangle^2]/N$ as a function of the thickness of the water film. For large wall–wall separations, this quantity

approaches the reduced isothermal compressibility of the fluid. In confinement, it can be used to estimate the activation barrier associated with a critical density fluctuation that triggers capillary evaporation. For this purpose, we treat the fluctuation in the number of molecules, $\delta N = N - \langle N \rangle$ at a fixed wall–wall separation, d , as a characteristic order parameter that changes along the liquid–vapor transition path.⁵⁶ For wall–wall distances $d = 13, 16, 19,$ or 22 Å, $\delta N_T \equiv (N_T - \langle N \rangle) = -27 \pm 3, -57 \pm 4, -73.5 \pm 6,$ or -90 ± 8 corresponded to situations where a pre-equilibrated system was equally likely to evaporate or to return to the average value of N in the liquid state, $\langle N \rangle$, characteristic of given separation, d . To a rough approximation, the states with $N = N_T$ can be identified with the peaks of the transition barriers. Values of N_T at each wall–wall separation, d , were determined from the outcome of a series of 10–20 open ensemble (μ, V, T) simulation runs performed for each of a set of different initial values of N . Initial states for these runs were generated by first equilibrating the system at a fixed initial value of $N < \langle N \rangle$ using closed (NVT) simulations. A trial run was interrupted when the system evaporated or regained the average liquid density characteristic of given d . Plotting the evaporation probability as a function of initial N enabled us to obtain N_T as the value of N where the prob-

ability of evaporation just fell below $1/2$. Knowing approximate values of N_T for a specified d , the work $\delta\Omega(d)$ associated with a perturbation $\delta N_T(d)$ was estimated from a truncated Taylor expansion of Ω in δN . Within an approximately Gaussian regime at small δN , the work required to perturb the system by δN , $\delta\Omega \propto \delta N^2$. However, at least the fourth order expansion is needed to capture the maximum in $\delta\Omega$ located at $\delta N = \delta N_T$ and the global minimum corresponding to the vapor phase, $\delta N_v \sim -\langle N \rangle$. In general, we can write $\delta\Omega/k_B T \sim a\delta N^2 + b\delta N^3 + c\delta N^4 + \dots$. If we ignore 5th and higher order terms, and using values for $a \equiv 1/2\langle \delta N^2 \rangle$ from Fig. 2(d), coefficients b and c follow from the positions of the extrema at δN_T and δN_v . The resulting activation barriers at $d=13, 16, 19,$ and 22 \AA are $3.5 \pm 0.5, 12 \pm 2, 18 \pm 3,$ and $26 \pm 6 k_B T$, respectively. These rough estimates,⁵⁷ in qualitative agreement with large scale on-lattice simulations,¹⁷ demonstrate the rapid increase of the activation barrier for capillary evaporation with pore width d and therefore rationalize the apparent stability of liquid water in mesoscopic apolar confinements encountered in practical situations. In particular, they help explaining the hysteresis observed in several surface-force measurements,^{10–12} as well as the pressure-induced slowdown of hydrophobic association between extended apolar domains of biopolymeric or colloidal solutes.

ACKNOWLEDGMENTS

One of the authors (D.B.) acknowledges former collaboration and helpful discussions with L. Blum, D. Henderson, A. Jamnik, A. Luzar, and M. S. Wertheim. This work was supported by the National Science Foundation and the U.S. Department of Energy (Basic Energy Sciences). The authors thank supercomputing centers, NPACI at San Diego and N.E.R.S.C. at LBNL for generous allocations of computing time.

- ¹G. Hummer, S. Garde, A. E. Garcia, and L. R. Pratt, *Chem. Phys.* **258**, 349 (2000).
- ²J. N. Israelachvili, *Intermolecular and Surface Forces* (Academic, London, 1992).
- ³D. F. Evans and H. Wennerstrom, *The Colloidal Domain: Where Physics, Chemistry, and Technology Meet* (Wiley, New York, 1999).
- ⁴K. Lum and A. Luzar, *Phys. Rev. E* **56**, R6283 (1997).
- ⁵K. Lum, D. Chandler, and J. D. Weeks, *J. Phys. Chem. B* **103**, 4570 (1999).
- ⁶T. M. Truskett, P. G. Debenedetti, and S. Torquato, *J. Chem. Phys.* **114**, 2401 (2001).
- ⁷V. V. Yaminsky, V. S. Yushchenko, E. A. Amelina, and E. D. Shchukin, *J. Colloid Interface Sci.* **96**, 301 (1983).
- ⁸V. S. Yushchenko, V. V. Yaminsky, and E. D. Shchukin, *J. Colloid Interface Sci.* **96**, 307 (1983).
- ⁹V. V. Yaminsky, E. A. Amelina, and E. D. Shchukin, *Colloids Surfaces* **6**, 68 (1983).
- ¹⁰P. M. Claesson and H. K. Christenson, *Science* **239**, 390 (1988).
- ¹¹J. L. Parker, P. M. Claesson, and P. Attard, *J. Phys. Chem.* **98**, 8468 (1994).
- ¹²H. Christenson and P. M. Claesson, *Adv. Colloid Interface Sci.* (in press).
- ¹³J. Forsman, B. Jonsson, and C. E. Woodward, *J. Phys. Chem.* **100**, 15005 (1996).
- ¹⁴V. V. Yaminsky and B. W. Ninham, *Langmuir* **9**, 3618 (1993).
- ¹⁵K. Lum and D. Chandler, *Int. J. Thermophys.* **19**, 845 (1998).
- ¹⁶A. Luzar and K. Leung, *J. Chem. Phys.* **113**, 5836 (2000).
- ¹⁷K. Leung and A. Luzar, *J. Chem. Phys.* **113**, 5845 (2000).
- ¹⁸M. Schoen, C. L. Rhykerd, J. H. Cushman, and D. J. Diestler, *Mol. Phys.* **66**, 1171 (1989).

- ¹⁹D. R. Berard, P. Attard, and G. N. Patey, *J. Chem. Phys.* **98**, 7236 (1993).
- ²⁰P. G. Bolhuis and D. Chandler, *J. Chem. Phys.* **113**, 8154 (2000).
- ²¹V. Talanquer and D. W. Oxtoby, *J. Chem. Phys.* **114**, 2793 (2001).
- ²²D. E. Ulberg and K. E. Gubbins, *Mol. Phys.* **84**, 1139 (1995).
- ²³B. Jonsson, *Chem. Phys. Lett.* **82**, 520 (1981).
- ²⁴D. Bratko and L. Blum, in *Hydrogen Bonded Liquids*, NATO ASI Series, edited by J. C. Dore and J. Teixeira (Kluwer Academic, Amsterdam, 1991), p. 185.
- ²⁵A. Delville, *J. Phys. Chem.* **97**, 9703 (1993).
- ²⁶J. R. Grigera, S. G. Kalko, and J. Fischbarg, *Langmuir* **12**, 154 (1996).
- ²⁷S. H. Lee and P. J. Rossky, *J. Chem. Phys.* **100**, 3334 (1994).
- ²⁸L. Perera, U. Essmann, and M. L. Berkowitz, *Langmuir* **12**, 2625 (1996).
- ²⁹J. Forsman, C. E. Woodward, and B. Jonsson, *J. Colloid Interface Sci.* **195**, 264 (1997).
- ³⁰K. A. T. Silverstein, A. D. J. Haymet, and K. A. Dill, *J. Am. Chem. Soc.* **120**, 3166 (1998).
- ³¹E. Spohr, A. Trokhymchuk, and D. Henderson, *J. Electroanal. Chem.* **450**, 281 (1998).
- ³²M. Meyer and H. E. Stanley, *J. Phys. Chem. B* **103**, 9728 (1999).
- ³³M. Ricci, F. Bruni, P. Gallo, M. Rovere, and A. K. Soper, *J. Phys.: Condens. Matter* **12**, A345 (2000).
- ³⁴I. Brovchenko, D. Paschek, and A. Geiger, *J. Chem. Phys.* **113**, 5026 (2000); I. Brovchenko, A. Geiger, and A. Oleinikova, *Phys. Chem. Chem. Phys.* **3**, 1567 (2001).
- ³⁵C. J. Lee, J. A. McCammon, and P. J. Rossky, *J. Chem. Phys.* **80**, 4448 (1984).
- ³⁶A. Luzar, D. Bratko, and L. Blum, *J. Chem. Phys.* **86**, 2955 (1987).
- ³⁷A. Wallqvist and B. J. Berne, *J. Phys. Chem.* **99**, 2893 (1995).
- ³⁸J. C. Shelley and G. N. Patey, *Mol. Phys.* **88**, 385 (1996).
- ³⁹M. Sakurai, H. Tamagawa, K. Ariga, T. Kunitake, and Y. Inoue, *Chem. Phys. Lett.* **289**, 567 (1998).
- ⁴⁰D. Bratko, L. Blum, and A. Luzar, *J. Chem. Phys.* **83**, 6367 (1985); L. Blum, F. Vericat, and D. Bratko, *ibid.* **102**, 1461 (1995).
- ⁴¹G. J. A. Vidugiris, J. L. Markley, and C. A. Royer, *Biochemistry* **34**, 4909 (1995); G. Panick, R. Malessa, R. Winter, G. Rapp, K. J. Frye, and C. A. Royer, *J. Mol. Biol.* **275**, 389 (1998).
- ⁴²G. Hummer, S. Garde, A. E. Garcia, M. E. Paulaitis, and L. R. Pratt, *Proc. Natl. Acad. Sci. U.S.A.* **95**, 1552 (1998); see also N. Hillson, J. N. Onuchic, and A. E. Garcia, *ibid.* **96**, 14848 (1999); A. Wallqvist, *J. Chem. Phys.* **96**, 1655 (1992).
- ⁴³H. J. C. Berendsen, J. P. M. Postma, W. F. van Gunsteren, and J. Hermans, in *Intermolecular Forces*, edited by B. Pullman (Reidel, Dordrecht, 1981), p. 331.
- ⁴⁴J. J. de Pablo, J. M. Prausnitz, H. J. Strauch, and P. T. Cummings, *J. Chem. Phys.* **93**, 7355 (1990).
- ⁴⁵J. Forsman, B. Jonsson, C. E. Woodward, and H. Wennerstrom, *J. Phys. Chem.* **101**, 4253 (1997).
- ⁴⁶According to Derjaguin approximation (Ref. 2) the force per unit area on planar walls, $P_l(d)$, is approximately equal to $1/(2\pi)$ times the derivative of the ratio $F(d)/R$ with respect to d where F is the measured force between curved surfaces with curvature radius R .
- ⁴⁷M. Mezei, *Mol. Phys.* **61**, 565 (1987).
- ⁴⁸J. C. Shelley and G. N. Patey, *J. Chem. Phys.* **102**, 7656 (1995).
- ⁴⁹J. Hautman and M. L. Klein, *Mol. Phys.* **75**, 379 (1992).
- ⁵⁰D. Bratko, D. J. Henderson, and L. Blum, *Phys. Rev. A* **44**, 8235 (1991); D. Bratko and D. Henderson, *Phys. Rev. E* **49**, 4140 (1994).
- ⁵¹T. Kuznetsowa and B. Kvamme, *Mol. Phys.* **97**, 423 (1999); J. Hermans, A. Pathiaseril, and A. Anderson, *J. Am. Chem. Soc.* **110**, 5982 (1988).
- ⁵²W. L. Jorgensen, J. Chandrasekhar, J. W. Madura, R. W. Impey, and M. L. Klein, *J. Chem. Phys.* **79**, 926 (1983).
- ⁵³A. A. Gardner and J. P. Valleur, *J. Chem. Phys.* **86**, 4162 (1987).
- ⁵⁴T. Ederth and Bo Liedberg, *Langmuir* **16**, 2177 (2000).
- ⁵⁵S. Ohnishi, V. V. Yaminsky, and H. K. Christenson, *Langmuir* **16**, 8360 (2000).
- ⁵⁶This appears a reasonable choice as long as the probability of multiple vapor pockets in the simulated system remains insignificantly low.
- ⁵⁷The present procedure is restricted to pore widths that are too low to provide a reliable scaling of the barrier height with separation d . Umbrella sampling techniques and the use of laterally increased systems capable of capturing long wavelength capillary phenomena (Refs. 4, 15, 16) have been proposed (Ref. 17) for more accurate calculations of the activation barriers.